ELSEVIER

Clinical Neurophysiology 115 (2004) 1697–1708

www.elsevier.com/locate/clinph

Electric field properties of two commercial figure-8 coils in TMS: calculation of focality and efficiency

Axel Thielscher[a,*], Thomas Kammer[b]

[a]Department of Psychiatry III, University of Ulm, Leimgrubenweg 12-14, D-89075 Ulm, BW, Germany
[b]Cortical Physiology Research Group, Department of Neurology, Hertie Institute for Clinical Brain Research, University of Tuebingen, Tuebingen, Germany

Accepted 21 February 2004

Available online 2 April 2004

Abstract

Objective: To compare two commonly used TMS coils, namely the Medtronic MC-B70 double coil and the Magstim 70 mm double coil, with respect to their electric field distributions induced on the cortex.

Methods: Electric field properties are calculated on a hemisphere representing the cortex using a spherical head model. The coil designs are characterised using several parameters, such as focality, efficiency and stimulation depth.

Results: Medtronic and Magstim coils exhibit similar focality values and stimulation depths, despite very different coil designs. However, the Medtronic coil is about 1.2 times more efficient compared to the Magstim coil. This difference corresponds to different motor and visual phosphene thresholds obtained in previous physiological studies, thereby validating the chosen coil modelling approach. Focality of the Medtronic coil changed less with varying coil–cortex distance compared to the Magstim coil, whereas both coils exhibited similar dependencies on changes in cortex radius.

Conclusions: The similar values for focality and stimulation depth indicate that both coil types should evoke similar physiological effects when adjusting for the different efficiencies. The different physiological thresholds of the two coils can be traced back to differences in coil design. Ideally, focality should depend neither on coil–cortex distance nor on cortex radius in order to allow for an inter-subject comparability. In particular, in motor mapping experiments the size of the resulting maps is affected by these two parameters. Consequently, they are at least partially the cause of the variability across subjects seen in these experiments.
© 2004 International Federation of Clinical Neurophysiology. Published by Elsevier Ireland Ltd. All rights reserved.

Keywords: Transcranial magnetic stimulation; Coil design; Electric field properties; Focality; Efficiency

1. Introduction

An important question in transcranial magnetic stimulation is to determine the site and size of stimulated cortex. For these purposes the geometries of the electric field induced by different coil types have been characterised by theoretical calculations (Jalinous, 1991; Ravazzani et al., 1996; Roth et al., 1990; Ruohonen, 1998; Zimmermann et al., 1996) or measurements of the electric currents induced in saline tanks (Maccabee et al., 1993). For example, using idealised coils consisting of one or two wire loops, it has been demonstrated that figure-8 coils allow for a more focused stimulation than simple round coils (Ravazzani et al., 1996). However, electric field calculations for the standard commercial figure-8 coils are still lacking. In the manuals of the manufactures only calculations of the induced magnetic field are given.

In the present paper we will compare the electric field properties of two commonly used figure-8 coils, namely the Magstim 70 mm (P/N 9790) and the Medtronic-Dantec MC-B70 double coils (Fig. 1). The field strengths and the field geometries induced on the cortex will be theoretically estimated using a spherical head model (Ilmoniemi et al., 1996; Sarvas, 1987) and compared with each other.

Furthermore, the differences between these fields and that of an idealised figure-8 coil will be demonstrated. Our results will be directly compared with measurements of motor and visual phosphene thresholds using the same coil types (Kammer et al., 2001a,b). This allows us to determine those coil parameters causing the physiological differences

* Corresponding author. Tel.: +49-731-5004-1253; fax: +49-731-5002-6751.

E-mail address: axel.thielscher@medizin.uni-ulm.de (A. Thielscher).

1388-2457/$30.00 © 2004 International Federation of Clinical Neurophysiology. Published by Elsevier Ireland Ltd. All rights reserved.
doi:10.1016/j.clinph.2004.02.019

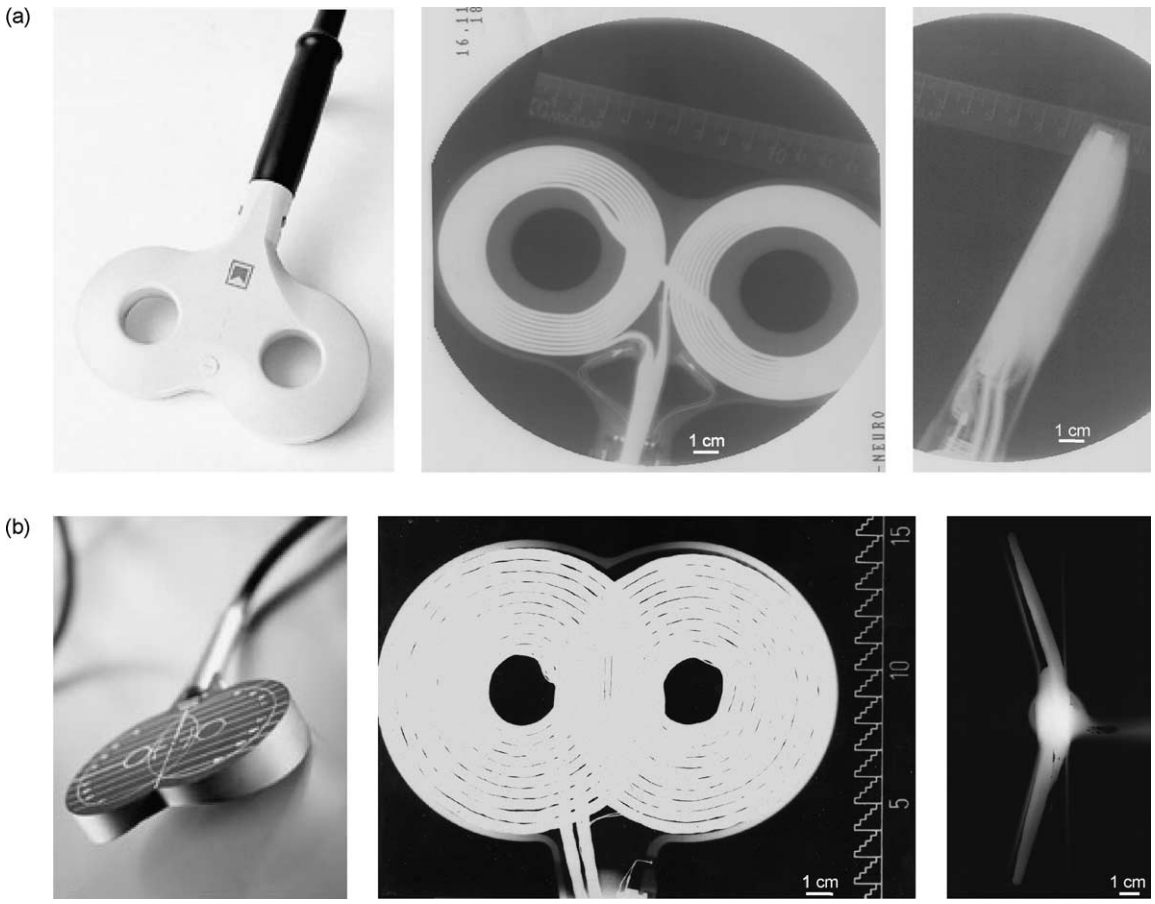

Fig. 1. Photos and X-ray pictures of (a) the Magstim figure-8 coil and (b) the Medtronic MC-B70 coil.

observed in the threshold measurements, in turn providing a link between predicted fields and physiological data.

Two parameters of a TMS coil are of particular interest: (i) the stimulation focality, and (ii) the efficiency, i.e. the amount of stimulator energy required to elicit a physiological response (e.g. a muscle action potential).

(i) The focality is normally defined as the cortical area in which the electric field strength exceeds a certain value relative to the maximum (e.g. the half maximum) (Roth et al., 1990). The smaller this area, the steeper the spatial decay of the field strength, in turn indicating a good focality. For a given position over the skull, the focality of a coil can be approximated using, e.g. a spherical head model and a hemisphere approximating the cortex.

(ii) The energy needed to get a physiological response when using a particular stimulator-coil-combination (i.e. the 'efficiency' of that combination) can be reliably measured using activation thresholds (Kammer et al., 2001b), but up to now it can hardly be determined by theoretical calculations. The efficiency not only depends on the maximum field strength induced in the cortex, but also on the stimulus waveform and duration. For a given coil position and a given rate of change of the coil current, the maximum field strength only depends on the coil geometry and can be approximated just as the focality using a theoretical head model. However, the effects of stimulus waveform and duration on the excitation of cortical neurons are poorly understood. Due to the complex neuronal dynamics and geometry as well as the interaction within the neural network, no realistic mathematical model exists up to now. For this reason, we focus on the efficiencies of the different coil geometries, but do not consider stimulus waveform and duration, which slightly differ between the stimulators of Magstim and Medtronic (Kammer et al., 2001b). We thereby characterise the efficiency of a coil by the maximum field strength value induced on the cortex, assuming the coil current to change by a rate of $dI/dt = 1$ A/s. The higher this value, the more effective the coil.

2. Methods

2.1. Spherical head model and dipole coil models

The induced electric field was estimated using the spherical head model described by Sarvas (1987). The model was implemented in MATLAB 6.0 (The Mathworks Inc., Natick, MA) using custom-made software. It allows to calculate the electric field which is induced in the head by a small magnetic dipole. In turn, the field of a coil can be

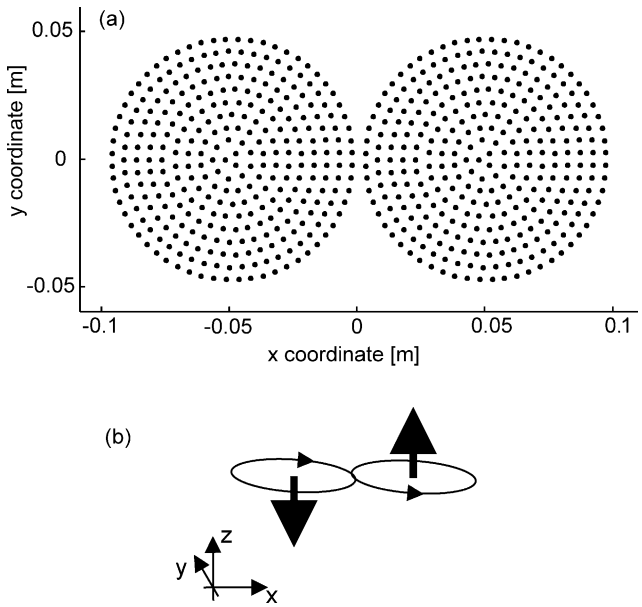

Fig. 2. (a) Dipole model of the idealised double coil ($r = 5.0$ cm). The dots indicate the positions of the dipoles. (b) The current counterrotates in the two wings. The z direction of the dipoles in one wing is therefore antiparallel to that of the dipoles in the other wing (indicated by the big arrows pointing up- and downwards).

described as a superposition of the fields of appropriately placed dipoles. A method of approximating a coil using dipoles is described in detail by Ravazzani et al. (1996). Briefly, the coil area is divided into subregions and the dipoles are placed perpendicular to the coil area in the centres of the subsurfaces. The dipoles are weighted by the coil current and the areas of the subregions. For example, the idealised figure-8 coil used in this paper can be modelled as two circular disks (radius $r = 5$ cm), which are divided into 10 rings each. Each ring is further divided into elements and the dipoles are placed in the centres of the elements, as shown in Fig. 2. The inner and outer radii of the rings as well as the number of elements of each ring are given in Table 1. The current counterrotates in the two wings. The direction of the dipoles in one wing is therefore antiparallel to that of the dipoles in the other wing.

The dipole models of the Magstim and Medtronic coils were created using X-ray pictures (Fig. 1). In contrast to an idealised coil, the coils of Magstim and Medtronic consist of several wire loops of different radii in each wing. In order to take this into account, the dipoles were weighted by the area of the subregion and the amount of current circling around them. For example, a dipole in the middle of a wing is surrounded by all wire loops of the wing and was therefore weighted by n times the coil current, whereby n represents the number of loops of that wing. In contrast, a dipole at the outer loop is surrounded by only one loop and consequently weighted by only once the coil current. A detailed specification of the model of the Medtronic coil can be found in Appendix A, the specification of the Magstim coil is given in Thielscher et al. (2002). Both coil dipole models were validated by comparison of calculated and measured electric fields induced in unbounded media (Appendix B).

Table 1
Dipole model of the idealised 50 mm double coil: inner and outer radii of the rings representing one wing and number of elements per ring

Inner radius (cm)	0.0	0.5	1.0	1.5	2.0	2.5	3.0	3.5	4.0	4.5
Outer radius (cm)	0.5	1.0	1.5	2.0	2.5	3.0	3.5	4.0	4.5	5.0
No. of elements	3	9	16	22	28	35	41	47	53	60

2.2. Focality

The focality of a coil was determined by calculating the electric field on a hemisphere representing the cortex (radius $r = 8$ cm; change of coil current $dI/dt = 1$ A/s; see right half of Fig. 3). The coil centre was placed 1.5 cm above it and the coil was oriented tangentially to it. The hemisphere was divided into subareas of 0.24 mm^2 and the electric field strength was calculated in the centre of each subarea. The total area of the hemisphere, in which the field strength exceeded, e.g. 50% of the maximum value, could then be simply determined by counting the number of subareas having a value of field strength greater than the given threshold and weighting the result with 0.24 mm^2. Assume, for example, that one stimulates a point-wise cortical area at motor threshold. Assume further, that the cortical excitation threshold is constant in the area under the coil and that the hemisphere is a sufficient approximation for the cortex surface. Then the area as determined above gives the approximate cortical area, which is stimulated when the stimulation level is raised to twice the motor threshold. Using the method described above, we systematically calculated the approximate cortical areas, which are stimulated at 110–200% intensity in relation to the threshold in steps of 10%.

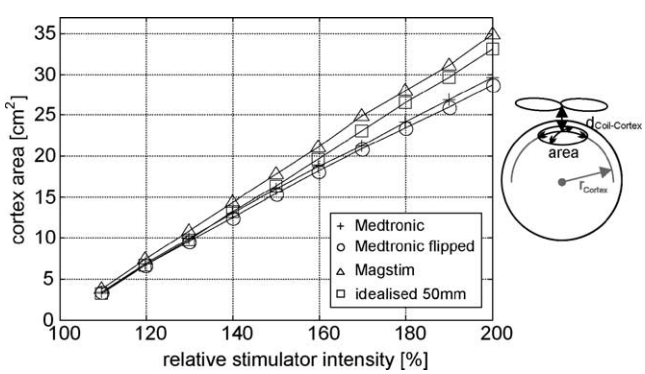

Fig. 3. Stimulated areas on a hemisphere for relative stimulation intensities ranging from 110 to 200% with three different figure-8 coils: Medtronic, Magstim and an idealized 50 mm coil. The Medtronic coil was calculated with two orientations: (1) 'normal' orientation with the wings angled along the convexity of the head, (2) 'flipped' with the wings pointing away from the convexity. The idealised coil consists of two single loops with a diameter of 50 mm each. Calculations are based on a sphere with $r_{Cortex} = 8$ cm, coil–cortex distance is $d = 1.5$ cm (inset on the right).

Subsequently, the influence of cortex radius on coil focality was tested by keeping the coil–cortex distance constant at 1.5 cm and systematically calculating focality values for cortex radii between 6 and 8.5 cm (step size 0.5 cm) using 120 and 200% relative stimulation intensities.

Finally, the impact of coil–cortex distance on focality was determined by keeping the cortex radius constant at 8 cm and varying the coil–cortex distance between 0.5 and 3 cm (step size 0.5 cm). Again, focality values for 120 and 200% relative stimulation intensities were calculated.

2.3. Decay of field strength with increasing stimulation depth

For figure-8 coils it is known that the maximum field strength is always located under the midpoint of the coil for all stimulation depth (Cohen et al., 1990). In order to determine the rate of decay of field strength with increasing stimulation depth, we thus calculated the electric field strength on a line perpendicular to the coil surface and starting in the midpoint of the coil (inset of Fig. 7a; change of coil current $dI/dt = 1$ A/s). We determined the field strength induced on that line for both the Medtronic and Magstim coils, respectively. Subsequently, we compared the efficiencies of their designs by taking the ratio of the obtained field strength values.

Finally, the steepness of field strength decay with increasing stimulation depth was characterised by determining the distances at which the field strength was 66 and 33%, respectively, of the maximum field strength value at the cortex with $r = 8.0$ cm.

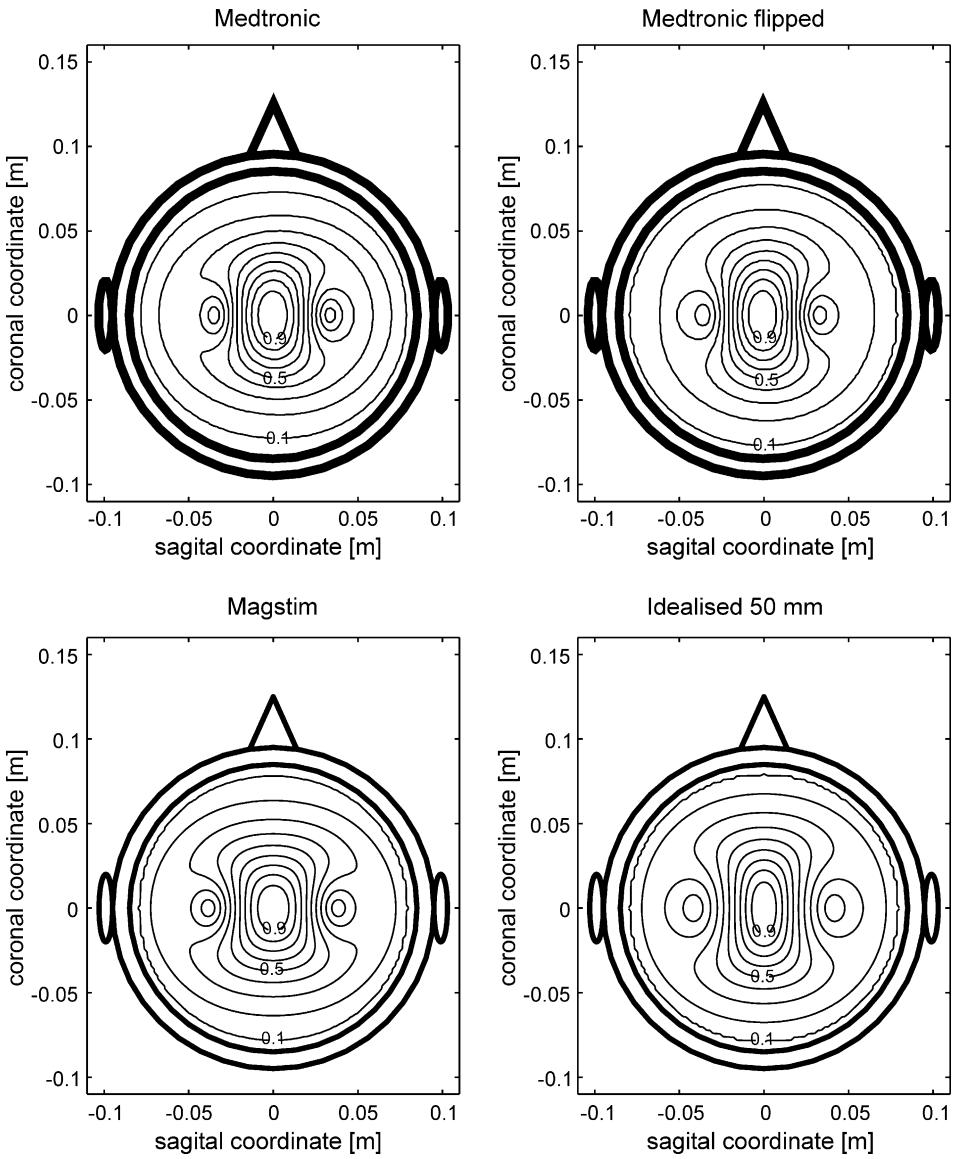

Fig. 4. Field geometries induced on the cortical hemisphere ($r_{Cortex} = 8$ cm, distance $d = 1.5$ cm). The view from above on the head model is shown. Coil configurations are the same as in Fig. 3. The field of the Medtronic coil is slightly asymmetric. Compared to the two commercial coils, the idealised double coil has a more oval field geometry.

3. Results

3.1. Focality and geometry of the induced electric fields

The estimated cortical areas which are stimulated at 110–200% relative intensities are depicted in Fig. 3. Unexpectedly, no large difference was found comparing the size of the areas stimulated by the Magstim coil and the Medtronic coil, although coil geometry largely differs. The two wings of the Magstim coil are side-by-side in one plane and they do not overlap. In contrast, the outer wings of the Medtronic coil are bend by angles of 16° (right wing) and 18.5° (left wing) towards the skull (Figs. 1b and A1). Furthermore, the wire loops overlap in the central part. Nevertheless, the Magstim coil was slightly less focal compared to the Medtronic coil (e.g. Magstim/Medtronic = 35/29.6 cm^2 at 200% relative intensity; Fig. 3). In order to determine the effect of the bends of the Medtronic coil on focality, we additionally flipped it and placed it up-side-down on the skull, with the bends pointing away from the skull and then repeated the calculation for that arrangement. The focality was slightly increased by that arrangement (e.g. about 0.9 cm^2 at 200% relative intensity with respect to the standard position).

The rather equal geometries of the fields induced on the hemisphere by the different coils was visualised by contour plots, with the contours depicting isolevel values of the field strength (Fig. 4). The greatest difference can be observed when comparing the geometries of commercial coils with the idealised coil, with wider and shorter field distributions of the commercial coils (due to the wire loops having a range of different radii) and a more oval shaped distribution

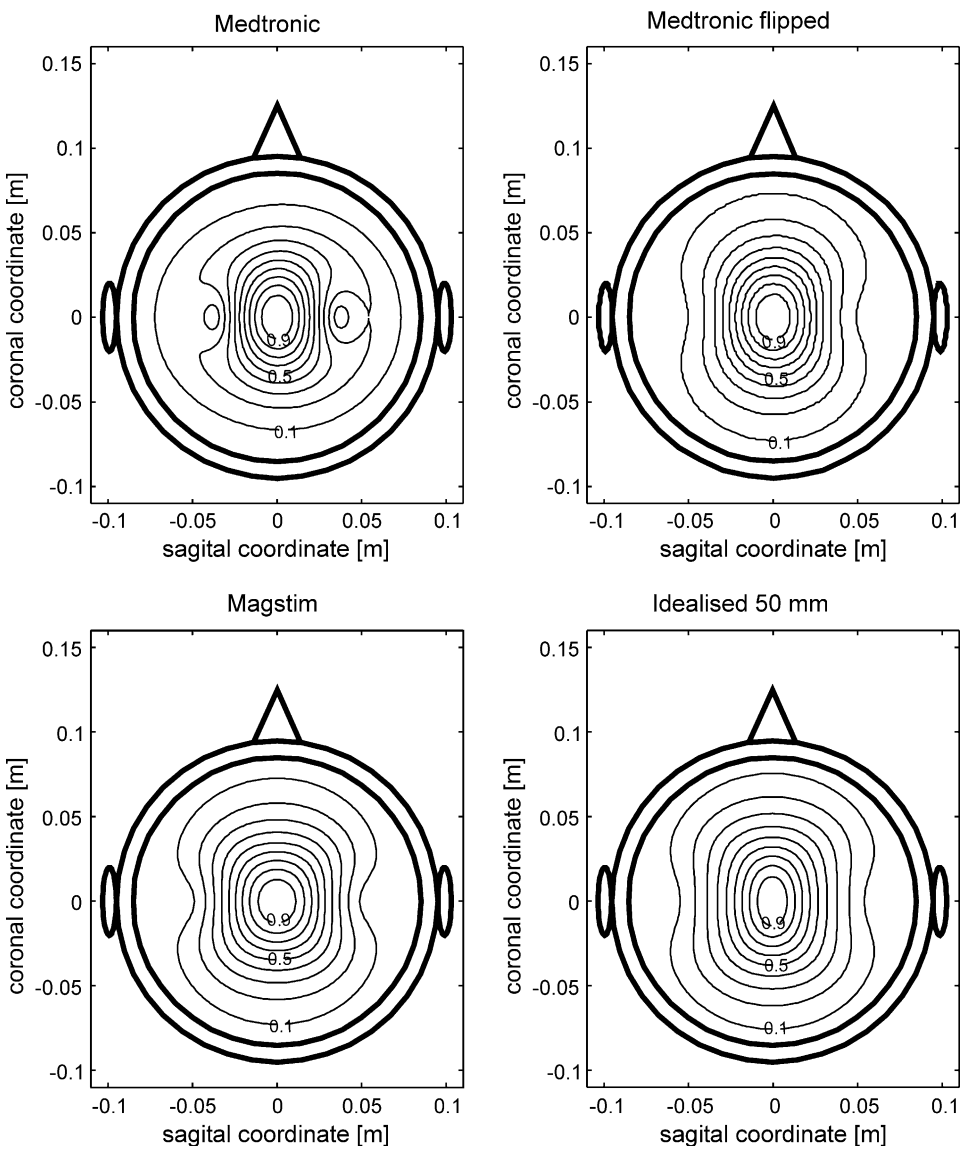

Fig. 5. Geometries of the vector potential induced on the cortical hemisphere (r_{Cortex} = 8 cm, distance d = 1.5 cm). The view from above on the head model is shown. Coil configurations are the same as in Fig. 3. The distributions of the vector potential are markedly less focal than the electric fields calculated using the spherical head model (compare Fig. 4).

of the idealised coil. The wire loops of the Medtronic coil overlap in the central part, resulting in unequal distances of the two wings to the cortex (Appendix A). However, these unequal distances do not remarkably shift the point of maximum field strength away from a position directly under the midpoint of the coil.

In order to visually demonstrate the substantial impact of the spherical boundary on the electric field distribution, we calculated the vector potential (i.e. the electric field in an unbounded medium) on the 'cortex' hemisphere (Fig. 5; compare with Fig. 4). In consequence, we concentrate on the spherical model in the current paper to ensure more realistic values of focality and efficiency (see Ravazzani et al. (1996) for a systematic investigation of the impact of different boundaries on the induced electric field).

3.2. Dependence of focality on coil–cortex distance

The focality of the idealised coil crucially depends on the coil–cortex distance, as can be seen in Fig. 6a (left). For a relative intensity of, e.g. 120%, the stimulated cortex area varies between 3.28 and 9.68 cm^2 for $d_{coil-cortex}$ of 0.5 and 3.0 cm, respectively. This is an increase of 295%. In contrast, the Medtronic coil has the most docile behaviour, with an increase from 6.5 to 7.5 cm^2 ($\approx$115%). The increase of the Magstim coil from 6.24 to 8.89 cm^2 ($\approx$142%) is markedly higher than that of the Medtronic coil. In general, the same differences between the coils can be observed for 200% relative stimulation intensity (Fig. 6a, right), indicating that they are maintained over the full range of relative intensities.

3.3. Dependence of focality on cortex radius

All coils show a moderate increase of stimulated area (i.e. a decrease of focality) with increasing cortex radius (Fig. 6b, left). At a relative stimulation intensity of 120%, the idealised coil has the highest increase from 5.6 to 6.8 cm^2 for cortex radii of 6 and 8.5 cm, respectively ($\approx$122%). The Medtronic and Magstim coils both have an increase of 119%. The focality values for 200% relative intensity (Fig. 6b, right) indicate that the observed increase of stimulated area with increasing cortex radius remains

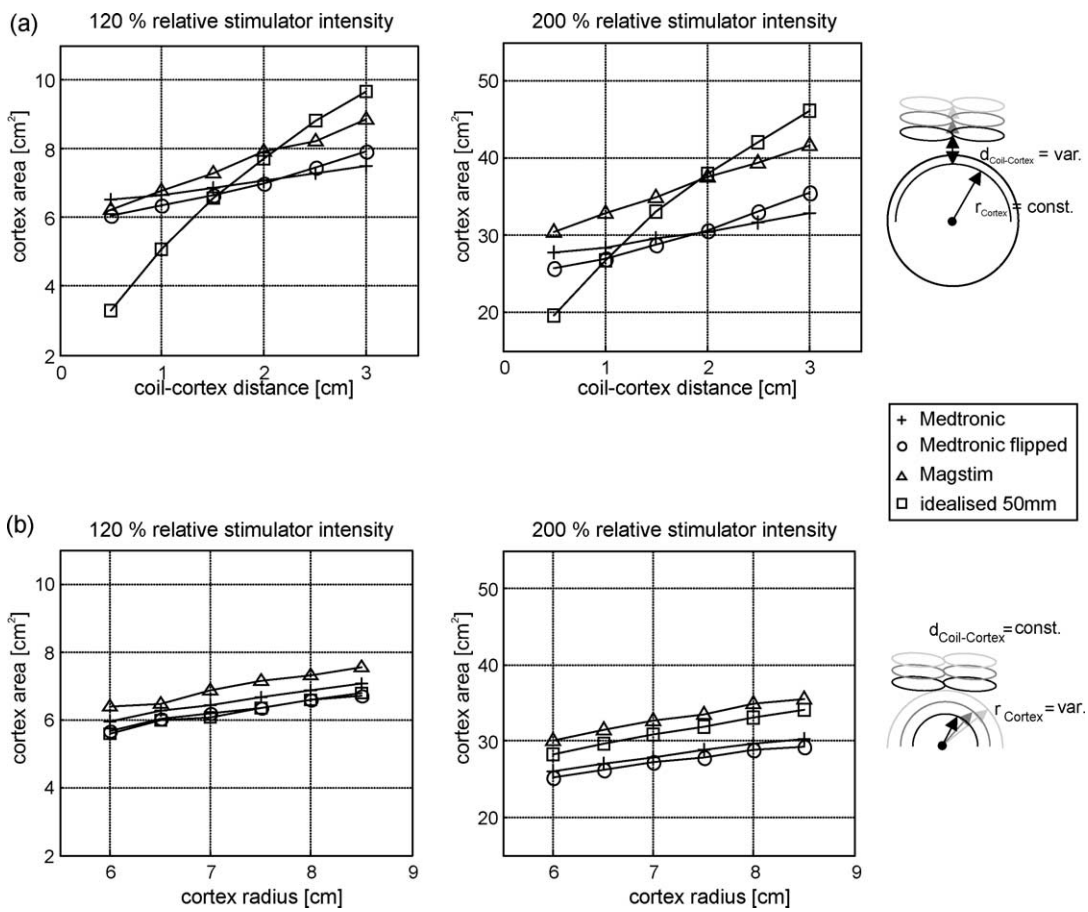

Fig. 6. (a) Dependence of coil focality on coil–cortex distance. For coil–cortex distances varying between 0.5 and 3 cm (see inset on the right, r_{Cortex} = const. = 8 cm), the cortex areas stimulated at 120% (left) and 200% (right) relative intensity are depicted. (b) Dependence of coil focality on cortex radius. For cortex radii varying between 6 and 8.5 cm, the cortex areas stimulated at 120% (left) and 200% (right) relative intensity are shown ($d_{Coil-Cortex}$ = const. = 1.5 cm). Coil configurations are the same as in Fig. 3.

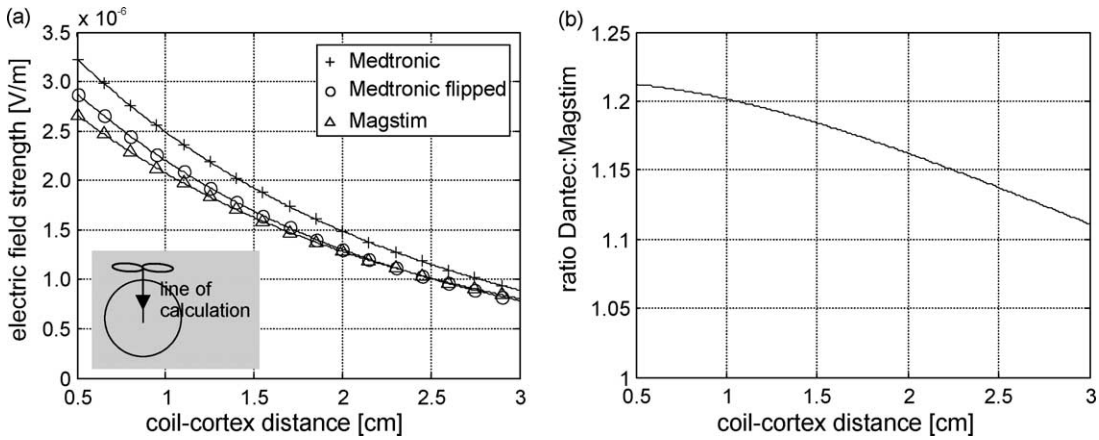

Fig. 7. Dependence of maximum induced field strength on stimulation depth. (a) The maximum field strength induced at coil–cortex distances between 0.5 and 3 cm (rate of change of coil current $dI/dt = 1$ A/s). The Medtronic coil achieves higher field strength values, i.e. a higher efficiency, compared to the Magstim coil. (b) Ratio between the maximum field strength induced by the Medtronic and Magstim coils in dependence of stimulation depth.

more or less constant over the full range of relative intensities.

3.4. Steepness of field strength decay and coil efficiency

The dependence of maximum field strength on stimulation depth is depicted in Fig. 7a ($dI/dt = 1$ A/s). The distances, at which the field strength is 66 and 33%, respectively, of the maximum at the cortex hemisphere with $r_{Cortex} = 8$ cm, are given in Table 2. As can be seen, all coils exhibit more or less the same decrease of field strength with increasing stimulation depth.

It applies in first approximation that the higher the number of wire loops of a coil, the higher its value of maximum field strength. Consequently, it makes no sense to compare the efficiency of an idealised coil consisting of only two wire loops with commercial coils, as it has clearly to be much lower. For that reason, we will focus on the two commercial coils in the following. Although the two coil designs result in quite equal focality values, their efficiencies differ from each other. For typical coil–cortex distances of 1.5 cm (Kozel et al., 2000; McConnell et al., 2001), the Medtronic coil is approximately 1.19 times more efficient than the Magstim coil (Fig. 7b). This is mainly a result of the bent wings, which can be seen when flipping the coil (line with circles in Fig. 7a).

4. Discussion

The main results of the present study are: (i) focality, i.e. the size of the electric field distribution does not largely differ between the two commonly used commercial coils Medtronic and Magstim, (ii) efficiency, i.e. the amount of the induced field for a given stimulator intensity is slighly higher for Medtronic compared to Magstim. This advantage diminishes with an increased coil–cortex distance.

4.1. Focality

Both the Medtronic and Magstim coils have focality values comparable to that of an idealised coil consisting of two wire loops each with a diameter of 10.0 cm. So their names (Medtronic MC-B70 and Magstim 70 mm double coil) referring to the mean loop diameters are rather misleading, as they do not allow any conclusions about their focality. However, coil focality defined as the cortical area stimulated at a certain above-threshold intensity is in first instance only a technical index (Roth et al., 1990). Several assumptions have to be made in order to allow for conclusions to be drawn about the size of the stimulated cortical area in reality:

- A sphere is an appropriate approximation of the cortex. In TMS, superficial brain structures are particularly stimulated rather than cortical tissue lying in deep sulci (Epstein et al., 1990; Rudiak and Marg, 1994). Consequently, this assumptions holds in first approximation at least for low relative stimulation intensities (e.g. 120% motor threshold).
- The size of the cortical area stimulated at threshold intensity (e.g. at motor threshold) is small and can be neglected. While this seems to hold for, e.g. muscle representations in M1 (Thielscher and Kammer, 2002), it

Table 2
Steepness of field strength decay with increasing stimulation depth

Field strength relative to the maximum at $r_{Cortex} = 8$ cm (%)	Distance to cortex hemisphere (cm)			
	Medtronic	Medtronic flipped	Magstim	Idealised 50 mm
66	0.79	0.79	0.86	0.82
33	2.15	2.17	2.34	2.34

is unclear for other cortical areas. The areas given in Fig. 3 are thus minimal values.

- The spherical head model describes the real electric field induced by a coil with sufficient accuracy. The limitations of the model and putative future developments are discussed in a separate section (see Section 4.4).
- The effect of current direction on the cortical activation threshold can be neglected (Kammer et al., 2001a,b; Mills et al., 1992; Pascual-Leone et al., 1994). The current direction in the focus of a figure-8 coil differs only slightly over different cortical positions (Fig. 1b of Thielscher and Kammer, 2002). So this assumptions seem to be uncritical for stimulation intensities slightly above threshold, but is clearly violated for higher intensities.
- The activation threshold is constant at different cortical positions when keeping the current direction constant. When comparing motor and visual thresholds no significant correlation could be observed (Kammer et al., 2003; Stewart et al., 2001), indicating that this assumption may be difficult to hold. However, for the calculation of the stimulated cortical area at low relative stimulation intensities, the activation threshold of only a few square centimeter of cortical tissue in the neighbourhood of the position of maximum field strength has to be constant. To our knowledge, no systematic investigation has been performed up to now addressing this question and consequently no reliable data is available.

Taken together, the areas depicted in Fig. 3 give a good idea about the size of stimulated cortical area at least for low relative stimulation intensities, provided that the last assumption holds to some degree. However, the discussion above is only a qualitative, but not a quantitative description of the sources of error.

4.2. Efficiency

For superficial cortical areas, the electric field induced by the Medtronic coil is approximately 1.19 times stronger than the field of the Magstim coil (Fig. 7b). In motor and visual phosphene threshold measurements (Kammer et al., 2001a, b) using the same figure-8 coils as in this paper, it was demonstrated that the Medtronic stimulator-coil-combination is 1.3 times (motor) and 1.24 times (phosphene) more effective than the Magstim stimulator-coil-combination. This indicates that the main part of the differences in efficiency observed in the physiological experiments can be traced back to the different coil designs. Several reasons are possible for the remaining part, namely the slightly different stimulus durations (Kammer et al., 2001b), noise in the physiological experiments as well as deviations between real and calculated electric field due to the simplified sphere model and slightly inaccurate coil dipole models (see below).

4.3. Dependence of focality on coil–cortex distance and cortex radius

Taken together, the Medtronic double coil exhibits the most moderate dependence of focality on variations of coil–cortex distance and/or cortex radius. This is, e.g. important for motor mapping experiments (Classen et al., 1998), in which the coil focality should differ as little as possible between subjects. However, our results clearly demonstrate that the differences in map size observed between subjects can at least partially be traced back to different coil–cortex distances and cortex radii.

4.4. Limitations of the sphere model

The problem of estimating how much our calculations using the sphere dipole model deviate from the electric fields induced in reality can be divided into two subquestions: (i) How well do the coil dipole models (which were created using X-ray pictures) describe the geometries of the wire loops of the real coils? (ii) How well does the spherical head model describe the real conductivity distribution in the human head?

(i) We systematically measured the voltages induced in a wire probe at several positions above the coil plane. Subsequently, we compared the results with theoretical values calculated using the coil dipole models and the equation describing the vector potential (i.e. the electric field in an unbounded medium) of a magnetic dipole (Appendix B). The mean deviations between measured and theoretical values were 3.5% (Medtronic) and 2.4% (Magstim), indicating that the dipole models describe the geometries of the real coils sufficiently good.

(ii) The limitations of spherical head models in magnetoencephalography (MEG) and TMS have been investigated in several theoretical as well as experimental studies. In such models, the radial electric field component is completely suppressed. It has been demonstrated by Sarvas (1987) that, in consequence, the conductivity of the sphere is not limited to a single value, but can have any spherically symmetric profile. The induced electric field in TMS and the external magnetic field in MEG, respectively, are not affected by radially symmetric changes in conductivity. In first approximation, such profiles resemble the changing conductivity levels of bone, liquor, grey and white matter. Furthermore, Ilmoniemi (1995) showed that the conductivity in radial direction can by an arbitrary function of location, i.e. can be radially anisotropic. He argues that radial anisotropies resemble conductivity changes due to fibre bundles in the white matter. In simulation studies, sphere models have been compared with more complex finite element models (FEM) of the head used in MEG. It was demonstrated that sphere models accurately describe the magnetic field distribution of a given dipole, with the exception of deep frontal and fronto-parietal areas (Hämäläinen and Sarvas, 1989; Ilmoniemi et al., 1999).

These results can be adopted for TMS using the reciprocity theorem describing the relation between MEG and TMS (Ilmoniemi et al., 1996). In a previous study (Thielscher and Kammer, 2002), we measured muscle action potentials and used them together with theoretically determined electric field distributions at several coil positions to determine the most likely cortical representation of a given target muscle. It could be demonstrated that the field strength values in the cortical muscle representation obtained by this method jittered with a variance of about 4% over the different coil positions. These results indicate that the spherical head model allows for a good approximation of the electric field of a TMS coil at least for superficial neural structures, e.g. at the top of a gyrus.

Future simulation studies might use more realistic conductivity distributions derived from, e.g. diffusion tensor measurements to bridge the remaining gap between theoretical and physiological studies. For example, Miranda et al. (2003) performed FEM simulations to determine the impact of a high conductivity inclusion (resulting, e.g. from a stroke) on the induced electric field in TMS. Furthermore, they calculated the electric field induced in a sphere with a constant anisotropic conductivity profile. Based on their results, they discussed the putative influence of varying conductivity levels in sulci due to the borders between grey and white matter and cerebro-spinal fluid being approximately perpendicular to the outer surface of the brain. Most interestingly, they argued that the resulting effects might be the cause of changing stimulation thresholds with changing coil orientations, as seen in physiological experiments (Kammer et al., 2001a,b, 2003).

4.5. The electric field induced by TMS coils: previous investigations

Several studies have been conducted to characterise the electric field induced by various types of TMS coils (Jalinous, 1991; Ravazzani et al., 1996; Roth et al., 1990; Ruohonen, 1998; Zimmermann and Simpson, 1996). Ravazzani et al. (1996) systematically investigated the influence of different head models (unbounded, semi-infinite and spherical volume conductors) on the induced field. They demonstrated the importance of using spherical models in order to get a realistic approximation of a coil's field. However, they concentrated on idealised double and round coils and did not use models of commercial coils. Roth et al. (1990) calculated the field distributions induced by several commercial round coils (of Cadwell and Novametrix) and one double coil (Cadwell) using a spherical head model and the same definition of focality as utilised in this paper. Our study serves as a completion of these previous approaches in that it helps to characterise the fields of two of the most frequently used commercial figure-8 coils. Furthermore, it gives a more complete characterisation of coil focality and tries to characterise the efficiency of their designs, in turn allowing for a direct comparison with data obtained by physiological measurements.

In conclusion our modelling approach allows a meaningful approximation of the induced electric field of the two common figure-8 coils investigated and accounts for differences in efficiency found in previous physiological studies. Since focality as well as stimulation depth of the two coils hardly differ, both coil types should evoke similar physiological effects when adjusting for the different efficiencies. As a consequence, results from studies performed with one of the two coils should be directly comparable to those using the other one. Future coil developments might consider the Medtronic design in order to increase efficiency resulting in reduced thermal load.

Acknowledgements

T.K. was supported by the DFG grant SFB 550/C5. The critical comments and helpful suggestions of the anonymous reviewers helped to improve the manuscript.

Appendix A

A.1. Dipole model of the medtronic MC-B70 double coil

The MC-B70 double coil consists of two wings with 10 wire loops each (Fig. 1b). The inner and outer radii of the loops are 1.2 and 5.4 cm, respectively. The wire is 3.5 mm thick. In the coil centre the windings of the two wings overlap. Next to the overlap, the windings of the left and right wings are bent by an angle of 18.5 and 16°, respectively. The thickness of the plastic chassis is 2 mm on the side attached to the head. Accordingly, two circular disks with radii of 5.4 cm were used to model the wings of the coil (Fig. A1). The disks were shifted by 3.2 cm in positive and negative x direction, respectively, to create the overlap. The distance between the wire loops and the outside of plastic chassis was taken into account by shifting the disks by 4.5 mm in negative z direction. Subsequently, a distance of 5 mm between the two disks in negative z direction was introduced. Each disk was divided into 12 rings and each ring was further divided into elements. The inner and outer radii of the rings, the number of elements of each ring, and the number of surrounding loops are given in Table A1. To account for the height of the wire, the circular disks were then divided into two planes each, which were shifted by 1.0 mm in positive and negative z direction, respectively. Consequently, a plane carries one-half of the current and all dipoles were weighted by a factor of one-half. The current counterrotates in the two wings. The direction of the dipoles in one wing is therefore antiparallel to that of the dipoles in the other wing. Finally, all dipoles in

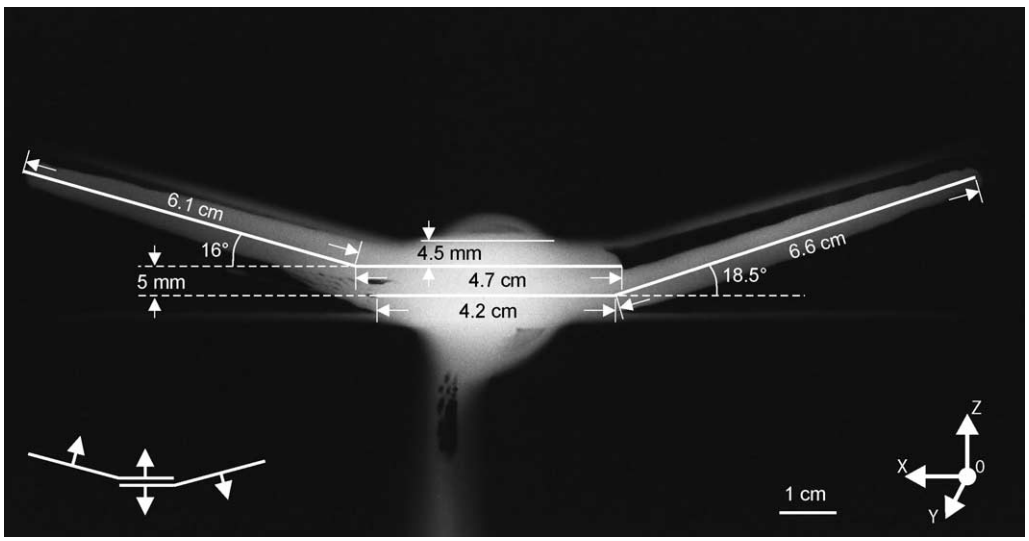

Fig. A1. Frontal view of the Medtronic dipole model as derived from the X-ray picture (radiological convention). The direction of the dipoles depends on the wing (bottom left).

the right disk (as shown in Fig. A1) with an X coordinate greater than 2.5 cm were bent up by 16° and all dipoles in the left disk with an X coordinate smaller than -2.0 cm were bent up by 18.5°.

Appendix B

B.1. Verification of the coil dipole models by measurement of the vector potential field

In order to verify the coil dipole models, we measured the voltage induced in a wire loop at several positions above the coil plane. We compared the obtained values with the vector potential fields of the TMS coils (see e.g. Ilmoniemi et al., 1999) which was theoretically determined using the dipole models.

A rectangular wire loop (5 mm × 11 mm) embedded in a block of acrylic glass was used as probe (Fig. B1a). It was attached to an oscilloscope which measured the induced voltage using a twisted wire pair. In order to minimize putative measurement errors due to voltage induced in the twisted wire pair (and not in the probe), the ending of the wire pair connected to the probe was arranged perpendicular to the coil plane. The short side of the probe was arranged parallel to the main (y-) axis of the coil, and the long side was parallel to the z-axis. For both the Magstim and Medtronic coils, monophasic pulses were used and the maximum voltage induced at the beginning of each pulse was determined. At each position, the measurement was repeated two times in order to detect putative outliers.

The probe was put on a panel of acrylic glass having a specific distance to the coil plane and systematically moved along the y- and x-axes of the coils in steps of 1 cm, resulting in a cross of measurement positions (Fig. B1b). The distance of the acrylic glass panel to the coil was systematically increased until the measured voltages became too weak. The position of the probe in relation to the coil was controlled using an optical tracking system (Flashpoint, Image Guided Technologies, USA). Altogether, measurements at 91 probe positions were performed per coil (Fig. B1c).

Along the crosses of measurement positions, the vector potential should be directed approximately parallel to the yz-plane of the coil. Consequently, the probe should measure zero voltage when it is rotated by 90° and its short side points in the direction of the coil's x-axis. In order to determine an upper limit of voltage induced in the twisted wire pair, we rotated the probe by 90° and repeated the measurements for the minimal coil-probe distance for each coil. The mean ratios between the voltages induced in the rotated and non rotated probe was 8.4% in case of the Medtronic coil and 4.3% in case of the Magstim coil.

Table A1
Dipole model of the medtronic MC-B70 double coil

Inner radius (cm)	0.0	0.6	1.2	1.7	2.1	2.5	2.9	3.3	3.7	4.1	4.6	5.0
Outer radius (cm)	0.6	1.2	1.7	2.1	2.5	2.9	3.3	3.7	4.1	4.6	5.0	5.4
No. of elements	3	9	12	16	20	24	28	32	36	40	44	48
No. of surrounding loops	10	10	10	9	8	7	6	5	4	3	2	1

Inner and outer radii of the rings representing one wing, number of elements per ring and number of surrounding loops.

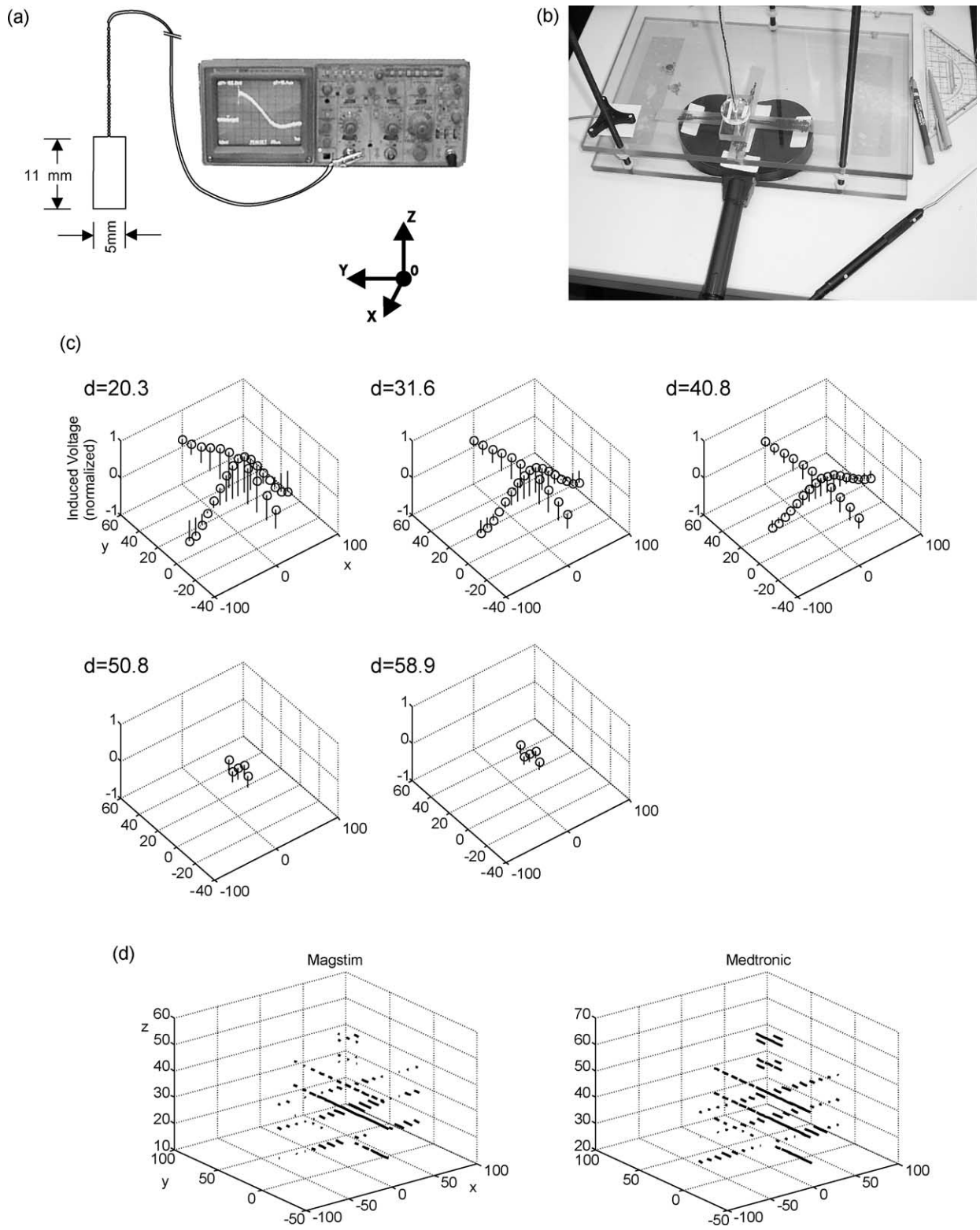

Fig. B1. (a) Dimensions and orientation of the rectangular wire probe. (b) Measurement setup. The wire probe was embedded in an acrylic glass block and put on an acrylic glass panel to control the distance to the coil plane. Positions were recorded using an optical tracking system. (c) Magstim coil: Distribution of the induced voltage in dependence on the probe position. The plots are normalized to the maximally induced voltage (at $x = 0$; $y = 0$; $d = 20.3$ in z-direction) and depict the distributions of the induced voltages in the xy-planes at the five measured coil-probe distances d. The normalised field strength are coded as line length in z-dimension. (d) Deviation between the measured and the theoretically calculated induced voltages in dependence on the probe position, collapsed across all coil-probe distances. The deviations are coded as line length (in y-direction), normalized to the maximum value across all positions. The deviation is approximately equally distributed across all probe-coil distances in case of the Medtronic coil. In case of the Magstim coil, the values are slightly enhanced for the probe-coil distance $d = 31.6$.

For each probe position, we calculated the theoretically induced voltage using the coil dipole models to numerically integrate the vector potential along the probe wire. Subsequently, the measured voltages and the theoretically induced voltages were normalized relative to their maximum values. The absolute difference between the normalized voltages was determined at each probe position to finally calculate the mean deviation between the measured and theoretical values over all positions (Fig. B1d). The mean deviation was 3.5% in case of the Medtronic coil and 2.4% for the Magstim coil, indicating that the dipole models describe the geometries of the real coils sufficiently good.

References

Classen J, Knorr U, Werhahn KJ, Schlaug G, Kunesch E, Cohen LG, Seitz RJ, Benecke R. Multimodal output mapping of human central motor representation on different spatial scales. J Physiol 1998;512(1): 163–79.

Cohen LG, Roth BJ, Nilsson J, Dang N, Panizza M, Bandinelli S, Friauf W, Hallett M. Effects of coil design on delivery of focal magnetic stimulation. Technical considerations. Electroencephalogr Clin Neurophysiol 1990;75:350–7.

Epstein CM, Schwartzberg DG, Davey KR, Sudderth DB. Localizing the site of magnetic brain stimulation in humans. Neurology 1990;40: 666–70.

Hämäläinen M, Sarvas J. Realistic conductivity geometry model of the human head for interpretation of neuromagnetic data. IEEE Trans Biomed Engng 1989;36(2):165–71.

Ilmoniemi RJ. Radial anisotropy added to a spherically symmetric conductor does not affect the external magnetic field due to internal sources. Europhys Lett 1995;30:313–6.

Ilmoniemi RJ, Ruohonen J, Virtanen J. Relationships between magnetic stimulation and MEG/EEG. In: translator, editor, editors. Advances in occupational medicine and rehabilitation, vol. 2(2). Pavia: Fondazione Salvatore Maugeri Edizioni; 1996.

Ilmoniemi RJ, Ruohonen J, Karhu J. Transcranial magnetic stimulation—a new tool for functional imaging of the brain. Crit Rev Biomed Engng 1999;27(3–5):241–84.

Jalinous R. Technical and practical aspects of magnetic nerve stimulation. J Clin Neurophysiol 1991;8(1):10–25.

Kammer T, Beck S, Erb M, Grodd W. The influence of current direction on phosphene thresholds evoked by transcranial magnetic stimulation. Clin Neurophysiol 2001a;112:2015–21.

Kammer T, Beck S, Thielscher A, Laubis-Herrmann U, Topka H. Motor thresholds in humans. A transcranial magnetic stimulation study comparing different pulseforms, current directions and stimulator types. Clin Neurophysiol 2001b;112:250–8.

Kammer T, Beck S, Puls K, Roether C, Thielscher A. Motor and phosphene thresholds: consequences of anisotropy. Suppl Clin Neurophysiol 2003; 56:198–203.

Kozel FA, Nahas Z, deBrux C, Molloy M, Lorberbaum JP, Bohning D, Risch SC, George MS. How coil–cortex distance relates to age, motor threshold, and antidepressant response to repetitive transcranial magnetic stimulation. J Neuropsychiatry Clin Neurosci 2000;12(3): 376–84.

Maccabee PJ, Amassian VE, Eberle LP, Cracco RQ. Magnetic coil stimulation of straight and bent amphibian and mammalian peripheral nerve in vitro: locus of excitation. J Physiol 1993;460:201–19.

McConnell KA, Nahas Z, Shastri A, Lorberbaum JP, Kozel FA, Bohning DE, George MS. The transcranial magnetic stimulation motor threshold depends on the distance from coil to underlying cortex: a replication in healthy adults comparing two methods of assessing the distance to cortex. Biol Psychiatry 2001;49:454–9.

Mills KR, Boniface SJ, Schubert M. Magnetic brain stimulation with a double coil: the importance of coil orientation. Electroencephalogr Clin Neurophysiol 1992;85:17–21.

Miranda PC, Hallett M, Basser PJ. The electric field induced in the brain by magnetic stimulation: a 3-D finite element analysis of the effect of tissue heterogeneity and anisotropy. IEEE Trans Biomed Engng 2003; 50(9):1074–85.

Pascual-Leone A, Cohen LG, Brasil-Neto JP, Valls-Solé J, Hallett M. Differentiation of sensorimotor neuronal structures responsible for induction of motor evoked potentials, attenuation in detection of somatosensory stimuli, and induction of sensation of movement by mapping of optimal current directions. Electroencephalogr Clin Neurophysiol 1994;93:230–6.

Ravazzani P, Ruohonen J, Grandori F, Tognola G. Magnetic stimulation of the nervous system: induced electric field in unbounded, semi-infinite, spherical and cylindrical media. Ann Biomed Engng 1996;24:606–16.

Roth BJ, Saypol JM, Hallett M, Cohen LG. A theoretical calculation of the electric field induced in the cortex during magnetic stimulation. Muscle Nerve 1990;13:734–41.

Rudiak D, Marg E. Finding the depth of magnetic brain stimulation: a re-evaluation. Electroencephalogr Clin Neurophysiol 1994;93:358–71.

Ruohonen J. Transcranial magnetic stimulation: modelling and new techniques. Helsinki: Helsinki University of Technology; 1998.

Sarvas J. Basic mathematical and electromagnetic concepts of the biomagnetic inverse problem. Phys Med Biol 1987;32(1):11–22.

Stewart LM, Walsh V, Rothwell JC. Motor and phosphene thresholds: a transcranial magnetic stimulation correlation study. Neuropsychologia 2001;39(4):415–9.

Thielscher A, Kammer T. Linking physics with physiology in TMS: a sphere field model to determine the cortical stimulation site in TMS. Neuroimage 2002;17:1117–30.

Zimmermann KP, Simpson RK. Slinky coils for neuromagnetic stimulation. Electroencephalogr Clin Neurophysiol 1996;101:145–52.